

Impurity transport study based on radial profile analysis of Fe L_α array with n=3-2 transitions of FeXVII to FeXXIV in LHD

X. L. HUANG¹, S. Morita^{1,2}, T. Oishi^{1,2}, M. Goto^{1,2}, H. M. Zhang¹, and I. Murakami^{1,2}

¹*Dept. of Fusion Sci., Graduate University for Advanced Studies, Toki 509-5292, Gifu, Japan*

²*National Institute for Fusion Science, Toki 509-5292, Gifu, Japan*

1. Introduction

Radial transport of impurity ions still remains several important issues in magnetically confined fusion devices, since the plasma performance is significantly affected by the radiation loss and fuel dilution caused by the impurity. In the Large Helical Device (LHD), the density profile can exhibit a variety of distributions of a peaked, flat or hollow shape, depending on plasma parameters such as B_t , T_e , and n_e . Therefore, it is of great importance to investigate the corresponding impurity transport in the plasma core of LHD [1-3]. As a typical phenomenon in the impurity transport it is reported that the impurity accumulation can be also observed in LHD as well as tokamaks, in which the transport is analyzed based on an assumption of the radial structure of convective velocity [4]. Formation of the hollow or flat density profile in the LHD is quite unique compared to the tokamak. Therefore, LHD plasmas give a good opportunity for studying the impurity transport through analysis of the radial structure in the transport coefficient, in particular, in relation to the density and temperature gradients.

Since iron is an intrinsic impurity in magnetically confined fusion plasmas, it is useful for a comprehensive study of the impurity transport under different plasma parameters or conditions. For the purpose, use of the Fe n=3-2 L_α transition array, emitted in narrow wavelength range of 10 – 18 Å, is of great advantage because the transition array consists of line emissions from iron ions in several charge states of Fe¹⁶⁺ through Fe²³⁺. In addition, these iron emissions have relatively strong emissivity and are distributed all over the plasma radius of LHD because the ionization energy of such ions ranging between 1 and 2 keV is nearly equal to the electron temperature in core region of LHD plasmas. Radial profiles of the Fe L_α emission have been measured with good quality by a space-resolved extreme-ultraviolet (EUV) spectrometer [5]. It is then possible to determine the profile of transport coefficients, i.e. the diffusion coefficient and the convective velocity, from the emissivity profile with the help of impurity transport simulation code.

2. Experimental setup

The EUV system used in the present study working in the wavelength range of 10-130Å mainly consists of an entrance slit, a spatial-resolution slit, a gold-coated concave varied-line-spacing (VLS) laminar-type holographic grating with a groove density of 2400 per mm and a charge-coupled device (CCD) detector with 1024×255 pixels ($26\mu\text{m} \times 26\mu\text{m}/\text{pixel}$). The EUV spectrometer is installed on a mid-plane port at the backside of a rectangular vacuum extension chamber. The elevation angle of the central viewing chord is exactly aligned to make possible the vertical profile measurement at upper half of the elliptical plasma, i.e. $Z = 0\text{--}50$ cm.

The iron spectrum including $n = 3\text{--}2$ L_α lines between 10 and 18 Å has been measured by injecting an iron impurity pellet [6]. A typical result is shown in Fig. 1. A lot of L_α transitions from highly ionized iron are observed in the spectrum. Since many iron lines are blended, the spectrum seems to be a pseudo-continuum. The emissivity profile is derived from the measured vertical profile based on a Fourier Method of Abel inversion [7]. The magnetic surface structure in LHD plasmas is calculated with variation moment equilibrium code (VMEC) [8]. Here, it should be pointed out that the magnetic flux surface calculated with the VMEC is also assumed outside the last close flux surface (LCFS) by extrapolating the magnetic surface contour at LCFS. Although the assumption may cause certain uncertainty, it does not strongly affect the emissivity peak inside the LCFS because the emissivity outside the LCFS is usually weak. The impurity density profile can be then calculated from the emissivity profile based on intensity coefficients obtained with the HULLAC code [9].

3. Transport simulation

A one-dimensional impurity transport code is employed to determine the transport coefficient. It is assumed that the impurity transport satisfies the following equation of

$$\Gamma_q = -D_q(r) \frac{\partial n_q}{\partial r} + V_q(r) n_q, \quad (1)$$

where Γ_q , n_q , D_q , V_q are the particle flux, the ion density, the diffusion coefficient and the convective velocity of impurity ions in the q th charge state, respectively. Positive and negative velocities stand for outward and inward convections, respectively.

Updated rate coefficients for ionization and recombination have been included in the present transport code [9-11]. With given transport coefficients and radial profiles of plasma parameters, the code yields the impurity ion density profile in all charge states as a function of time. The transport coefficient near the emissivity peak can be determined by comparing the emissivity profile between the experiment and the simulation. In order to determine the transport coefficient at the whole plasma radius, the iron emission is simultaneously analyzed at several charge states. The minimization of deviation between measured and simulated impurity profiles can determine the transport coefficient profile.

4. Transport analysis of discharges with hollow density profile

Figure 2 shows the result of transport analysis for a high-density hydrogen discharge with Fe pellet injection. The density profile is clearly hollow. The magnetic axis position is 3.6m and the toroidal field is 2.75T. Here, the radial structure of the transport coefficient is analyzed using measured density profiles of FeXVII through FeXXII. The transport code can well reproduce the profiles, as denoted by solid line in Fig. 2(a). The transport coefficients determined here are shown in Fig. 2(b). The diffusion coefficient gradually increases from the plasma center to the edge, while the convection velocity changes its direction from outward to inward. The transition point is around $\rho=0.82$ of which the value is equal to the peak position of the hollow density profile. Since the impurity density is less than 10^{-4} to the electron density, the proton density should be nearly equal to the electron density. Therefore,

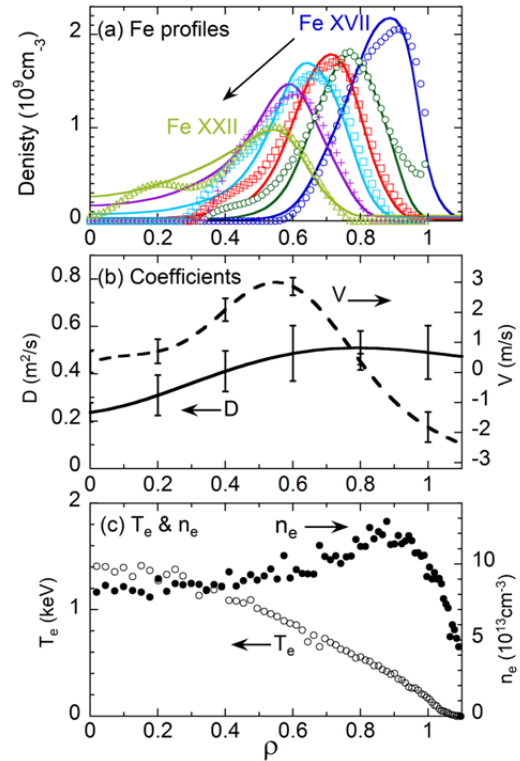


FIG. 2. Experimental (symbols) and simulated (solid lines) profiles of (a) FeXVII through FeXXII, (b) diffusion coefficient (solid line) and convective velocity (dashed line) and (c) T_e (open circles) and n_e (solid circles).

the result suggests the convection is related to the gradient of ion density profile. This is in accordance with the neoclassical theory of the impurity transport which predicts that the impurity concentrates in the peak position of the ion density. In fact, the impurity further concentrates in the plasma edge when the density profile becomes hollower, as shown in Fig. 3. In this discharge, the outward convection velocity is even larger than that in Fig. 2. The result corresponds to the hollower density profile in spite of the relatively low density discharge.

In conclusion, a large outward convection velocity is observed in the plasma center when a hollow density profile occurs. The convection velocity changes the direction at radial location where the density gradient is negative. No significant change in the diffusion coefficient along the plasma radius is observed.

Acknowledgements

The authors thank all members of the LHD experimental group for their technical supports. This work was partially carried out under the LHD project financial support (NIFS14ULPP010), the JSPS KAKENHI Grant Number 23340183 and JSPS-NRF-NSFC A3 Foresight Program in the field of Plasma Physics (NSFC: No. 11261140328, NRF: No. 2012K2A2A6000443).

References

- [1] S. Morita *et al.*, *Plasma Sci. Technol.* **8**, 55 (2006).
- [2] Y. Nakamura *et al.*, *Nucl. Fusion* **43**, 219 (2003).
- [3] M. Yoshinuma *et al.*, *Nucl. Fusion* **49**, 062002 (2009).
- [4] C. F. Dong *et al.*, *Plasma Sci. Technol.* **15**, 230 (2013).
- [5] X. L. Huang *et al.*, *Rev. Sci. Instrum.* **85**, 043511 (2014).
- [6] R. Katai *et al.*, *Jpn. J. Appl. Phys.* **46**, 3667 (2007).
- [7] G. Pretzler *et al.*, *Z. Naturforsch.* **47a**, 955 (1992).
- [8] S. P. Hirshman *et al.*, *Comput. Phys. Commun.* **43**, 143 (1986).
- [9] A. Bar-Shalom *et al.*, *J. Quant. Spectrosc. Radiat. Trans.*, **71**, 169 (2001).
- [10] N. R. Badnell, *Astrophys. J. Suppl. Ser.* **167**, 334 (2006).
- [11] N. R. Badnell *et al.*, *Astron. Astrophys.* **406**, 1151 (2003).
- [12] K. P. Dere, *Astron. Astrophys.* **466**, 771 (2007).

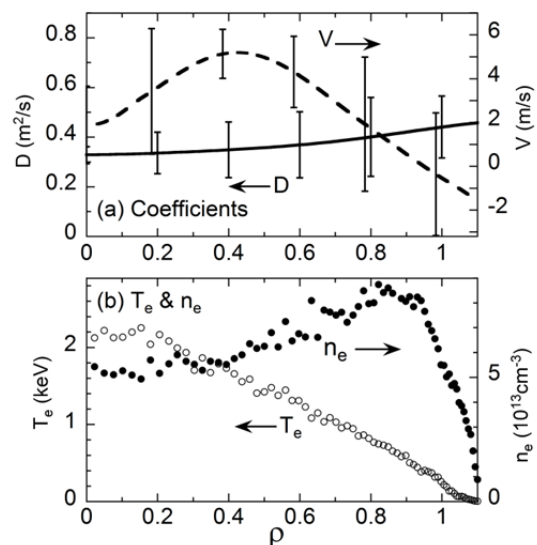


FIG. 3. (a) Diffusion coefficient (solid line) and convective velocity (dashed line) and (b) T_e (open circles) and n_e (solid circles).